Scientific Research Publishing

9International Journal of Astronomy and Astrophysics, 2025, 15(1), 19-42
https://www.scirp.org/journal/ijaa
ISSN Online: 2161-4725
ISSN Print: 2161-4717

New Probability Distributions in Astrophysics: XIV. Truncation of the Modified Lognormal Distribution

Lorenzo Zaninetti

Physics Department (Retired), University of Turin, Turin, Italy
Email: l.zaninetti@alice.it

How to cite this paper: Zaninetti, L. (2025) New Probability Distributions in Astrophysics: XIV. Truncation of the Modified Lognormal Distribution. *International Journal of Astronomy and Astrophysics*, **15**, 19-42.
https://doi.org/10.4236/ijaa.2025.151003

Received: November 24, 2024
Accepted: February 3, 2025
Published: February 6, 2025

Abstract

In order to introduce left and right truncated versions of the modified lognormal with a power-law distribution, we derive its probability density function, its distribution function, its average value, its second moment of the origin, its variance, how to randomly generate its values, the maximum likelihood and the nonlinear least squares estimators for its three unknown parameters. It is then applied to five clusters of stars, to the mass function for stars, and to one catalog for the masses of the galaxies.

Keywords

Stars: Normal, Stars: Luminosity Function, Mass Function Stars: Statistics

1. Introduction

The field of astrophysics routinely applies the standard distribution of probabilities in different environments such as the distributions in mass and luminosity of stars and galaxies. The normal or Gaussian distribution, introduced by Pearson in 1902 [1] is in principle the first distribution to be considered, but due to the fact that the mass and luminosity are always positive, it presents an inconvenience. The half Gaussian and the truncated half Gaussian [2] are defined for positive values of the variate and therefore can be used to model the stars' heights above the Galactic plane. Another example is the case of the gamma family for the luminosity function for galaxies, which started with Schechter in 1976 [3]. An improvement in the fit of the luminosity function for galaxies has been made by considering the generalized gamma distribution [4] and the truncated generalized gamma distribution [5]. Another distribution useful in astrophysics is the lognormal, which dates back to Galton and McAlister in 1879 [6] [7]. Other names are also used for the lognormal, such as Cobb-Douglas in 1928 [8], Gibrat in 1931 [9] and logarithmic-normal in 1919 [10]. We now review some recent applications of the lognormal distribution: to model the distribution function of the flux and the dependence of the standard deviation of the flux on the mean flux [11], the Fermi data of the blazar 3FGL J0730.2-1141, showing that its γ-ray flux is consistent with a lognormal distribution [12], data analysis of the results of the three-dimensional hydro-dynamical simulations of shocks [13], analysis of the distribution properties of the areas of sunspots [14], and the distribution of γ-ray flux and the statistical characteristics of a large sample of 1414 variable blazars from the Fermi-LAT LCR catalog [15]. We now pose some questions not yet solved.

1) Is it possible to introduce the effect of truncation in the modified lognormal with a power-law (MLP) distribution?

2) Can the truncated MLP distribution explain the initial mass function for the stars which usually is reported between $10^{-2} M/\mathcal{M}_\odot < 10^2$?

In order to answer these questions, we review the following distributions in Section 2: the lognormal, the truncated lognormal, and the double Pareto-lognormal. Section 3 reviews the statistics connected with the MLP distribution and Section 4 introduces the truncated MLP. Section 5 applies the new and old distributions to five clusters of stars and one of galaxies and Section 6 derives the parameters of the truncated MLP for the mass function of stars.

2. The Lognormal Family

In the following, PDF means probability density function and DF distribution function. The function $\mathrm{erf}(x)$, the error function, is defined in **Appendix A**.

We now review the lognormal distribution, the truncated lognormal distribution and the double Pareto-lognormal distribution.

2.1. The Lognormal Distribution

Let X be a random variable taking values x in the interval $[0,\infty]$; the first definition for the lognormal PDF, following [16] or formula (14.2) in [17], is

$$f(x:m,\sigma)=\frac{1}{x\sigma\sqrt{2\pi}}\exp\frac{-\left[\ln(x/m)\right]^2}{2\sigma^2}. \tag{1}$$

The average value, $E(m,\sigma)$, is

$$E(m,\sigma)=m\mathrm{e}^{\frac{\sigma^2}{2}}, \tag{2}$$

and the distribution function, $F(x:m,\sigma)$,

$$F(x:m,\sigma)=\frac{1}{2}-\frac{\mathrm{erf}\left(\frac{\sqrt{2}\left(\ln(m)-\ln(x)\right)}{2\sigma}\right)}{2}. \tag{3}$$

The second definition is

$$f(x:\mu,\sigma)=\frac{1}{x\sigma\sqrt{2\pi}}\exp\frac{-(\ln x-\mu)^2}{2\sigma^2}, \quad (4)$$

where $m=\exp\mu$ and $\mu=\ln m$. The average value, $E(\mu,\sigma)$ is

$$E(\mu,\sigma)=\mathrm{e}^{\frac{\sigma^2}{2}+\mu}, \quad (5)$$

and the distribution function, $F(x:\mu,\sigma)$,

$$F(x:\mu,\sigma)=\frac{1}{2}+\frac{\operatorname{erf}\left(\frac{\sqrt{2}(\ln(x)-\mu)}{2\sigma}\right)}{2}. \quad (6)$$

2.2. The Truncated Lognormal Distribution

Let X be a random variable defined in $[x_l,x_u]$; the truncated lognormal PDF (f_T) is based on the first definition of the lognormal as given by Equation (1)

$$f_T(x:m,\sigma,x_l,x_u)= \quad (7)$$

$$\frac{\sqrt{2}\mathrm{e}^{-\frac{1}{2}\frac{1}{\sigma^2}\left(\ln\left(\frac{x}{m}\right)\right)^2}}{-\sqrt{\pi}\sigma\left(\operatorname{erf}\left(\frac{1}{2}\frac{\sqrt{2}}{\sigma}\ln\left(\frac{x_l}{m}\right)\right)-\operatorname{erf}\left(\frac{1}{2}\frac{\sqrt{2}}{\sigma}\ln\left(\frac{x_u}{m}\right)\right)\right)x}, \quad (8)$$

where m is the scale parameter, σ is the shape parameter, x_l denotes the minimal value, and x_u denotes the maximal value. The introduction of the following coefficients allows a compact notation

$$a_1=\frac{1}{2}\frac{\sqrt{2}\left(-\sigma^2+\ln(x_l)-\ln(m)\right)}{\sigma},$$

$$a_2=\frac{1}{2}\frac{\sqrt{2}\left(\sigma^2+\ln(m)-\ln(x_u)\right)}{\sigma},$$

$$a_3=\frac{1}{2}\frac{\sqrt{2}\left(\ln(x_l)-\ln(m)\right)}{\sigma},$$

$$a_4=\frac{1}{2}\frac{\sqrt{2}\left(-\ln(x_u)+\ln(m)\right)}{\sigma},$$

$$a_5=\frac{1}{2}\frac{\sqrt{2}\left(-2\sigma^2+\ln(x_l)-\ln(m)\right)}{\sigma},$$

$$a_6=\frac{1}{2}\frac{\sqrt{2}\left(2\sigma^2+\ln(m)-\ln(x_u)\right)}{\sigma},$$

$$a_7=\frac{1}{2}\frac{\sqrt{2}\left(-2\sigma^2+\ln(x_u)-\ln(m)\right)}{\sigma},$$

$$a_8=\frac{1}{2}\frac{\sqrt{2}\left(\ln(x_u)-\ln(m)\right)}{\sigma}.$$

In this compact notation, the PDF is

$$f_T(x:m,\sigma,x_l,x_u)=\frac{-\sqrt{2}\mathrm{e}^{-\frac{1}{2}\frac{1}{\sigma^2}\left(\ln\left(\frac{x}{m}\right)\right)^2}}{\sqrt{\pi}\sigma\left(\mathrm{erf}(a_3)-\mathrm{erf}(a_8)\right)x}, \tag{9}$$

the DF is

$$F_T(x:m,\sigma,x_l,x_u)=\frac{-\mathrm{erf}\left(\frac{1}{2}\frac{\sqrt{2}}{\sigma}\ln\left(\frac{x}{m}\right)\right)+\mathrm{erf}(a_3)}{\mathrm{erf}(a_3)-\mathrm{erf}(a_8)}, \tag{10}$$

and the mean, $E_T(m,\sigma,x_l,x_u)$, is

$$E_T(m,\sigma,x_l,x_u)=\frac{\mathrm{e}^{\frac{1}{2}\sigma^2}m\left(\mathrm{erf}(a_1)+\mathrm{erf}(a_2)\right)}{\mathrm{erf}(a_3)+\mathrm{erf}(a_4)}. \tag{11}$$

More details can be found in [18].

2.3. The Double Pareto-Lognormal Distribution

The double Pareto lognormal distribution as represented by formula (22) in [19] has PDF

$$\begin{aligned}
&f(x:\alpha,\beta,\mu,\sigma)\\
&=\frac{1}{2(\alpha+\beta)x}\times\left(-\alpha\left(x^{\beta}\mathrm{e}^{\frac{1}{2}\beta^2\sigma^2-\beta\mu}\mathrm{erf}\left(\frac{\left(\beta\sigma^2-\mu+\ln(x)\right)\sqrt{2}}{2\sigma}\right)\right.\right.\\
&\left.\left.-x^{\beta}\mathrm{e}^{\frac{1}{2}\beta^2\sigma^2-\beta\mu}+\left(\mathrm{erf}\left(\frac{\left(\alpha\sigma^2+\mu-\ln(x)\right)\sqrt{2}}{2\sigma}\right)-1\right)x^{-\alpha}\mathrm{e}^{\frac{1}{2}\alpha^2\sigma^2+\alpha\mu}\right)\right)\beta
\end{aligned} \tag{12}$$

where α and β are the Pareto coefficients for the upper and the lower tail, respectively, while μ and σ are the lognormal body parameters. The DF is

$$\begin{aligned}
&F(x:\alpha,\beta,\mu,\sigma)\\
&=\frac{1}{2\alpha+2\beta}\times\left(x^{-\alpha}\beta\mathrm{e}^{\frac{1}{2}\alpha^2\sigma^2+\alpha\mu}\mathrm{erf}\left(\frac{\left(\alpha\sigma^2+\mu-\ln(x)\right)\sqrt{2}}{2\sigma}\right)\right.\\
&-\mathrm{e}^{\frac{1}{2}\beta^2\sigma^2-\beta\mu}\alpha x^{\beta}\mathrm{erf}\left(\frac{\left(\beta\sigma^2-\mu+\ln(x)\right)\sqrt{2}}{2\sigma}\right)-x^{-\alpha}\beta\mathrm{e}^{\frac{1}{2}\alpha^2\sigma^2+\alpha\mu}\\
&+\mathrm{e}^{\frac{1}{2}\beta^2\sigma^2-\beta\mu}\alpha x^{\beta}+\alpha\mathrm{erf}\left(\frac{\sqrt{2}\left(-\mu+\ln(x)\right)}{2\sigma}\right)\\
&\left.+\beta\mathrm{erf}\left(\frac{\sqrt{2}\left(-\mu+\ln(x)\right)}{2\sigma}\right)+\alpha+\beta\right),
\end{aligned} \tag{13}$$

and the mean $E(\alpha,\beta,\mu,\sigma)$, defined for $\alpha>1$, is

$$E(\alpha,\beta,\mu,\sigma)=\frac{\mathrm{e}^{\frac{\sigma^2}{2}+\mu}\alpha\beta}{(\alpha-1)(\beta+1)}, \tag{14}$$

see formula (25) in [19].

3. The MLP Distribution

The modified lognormal with a power-law (MLP) defined in the interval $[0,\infty]$ has the following PDF

$$f(x:\alpha,\sigma,\mu)=\frac{x^{-1-\alpha}\operatorname{erfc}\left(\frac{\sqrt{2}\left(\alpha\sigma-\frac{\ln(x)-\mu}{\sigma}\right)}{2}\right)\alpha}{2\mathrm{e}^{-\frac{1}{2}\alpha^2\sigma^2-\alpha\mu}}, \tag{15}$$

see formula (14) in [20]. Its DF is

$$F(x:\alpha,\sigma,\mu)=-\frac{\operatorname{erfc}\left(\frac{\sqrt{2}\left(\alpha\sigma^2-\ln(x)+\mu\right)}{2\sigma}\right)x^{-\alpha}\mathrm{e}^{\frac{1}{2}\alpha^2\sigma^2+\alpha\mu}}{2}+1-\frac{\operatorname{erfc}\left(\frac{\sqrt{2}\left(\ln(x)-\mu\right)}{2\sigma}\right)}{2}, \tag{16}$$

see formula (16) in [20]. The first moment or mean, $E(\alpha,\sigma,\mu)$, is defined for $\alpha>1$:

$$E(\alpha,\sigma,\mu)=\frac{\alpha\mathrm{e}^{\frac{\sigma^2}{2}+\mu}}{\alpha-1}, \tag{17}$$

see formula (19) in [20].

The variance, $Var(\alpha,\sigma,\mu)$, is defined for $\alpha>2$:

$$Var(\alpha,\sigma,\mu)=-\frac{\alpha^2\left(\mathrm{e}^{\frac{\sigma^2}{2}+\mu}\right)^2}{(\alpha-1)^2}+\frac{\alpha\mathrm{e}^{2\sigma^2+2\mu}}{\alpha-2}, \tag{18}$$

see formula (21) in [20]. The mode should be evaluated numerically. The random generation of the variate X of the truncated MLP is obtained by solving the following nonlinear equation in x:

$$F(x:\alpha,\sigma,\mu)=R, \tag{19}$$

where R is the unit rectangular variate. We give an approximation for the error function among eleven others; see **Table 1** in [21] for more details,

$$\operatorname{erf}(x)\approx\tanh\left(\frac{39x}{2\sqrt{\pi}}-\frac{111\arctan\left(\frac{35x}{111\sqrt{\pi}}\right)}{2}\right), \tag{20}$$

see formula (3.1) in [22]. With the above approximation, the PDF is

$$f(x:\alpha,\sigma,\mu) \approx \frac{1}{2\mathrm{e}^{-\frac{1}{2}\alpha^2\sigma^2-\alpha\mu}} \times \left(-x^{-1-\alpha} \left(\tanh\left(\frac{39\sqrt{2}\left(\alpha\sigma^2 - \ln(x) + \mu\right)}{4\sigma\sqrt{\pi}} - \frac{111\arctan\left(\frac{35\sqrt{2}\left(\alpha\sigma^2-\ln(x)+\mu\right)}{222\sigma\sqrt{\pi}}\right)}{2} \right) - 1 \right) \alpha \right). \tag{21}$$

An example of such an approximation is presented in **Figure 1**, which has a maximum percentage error of 7%. The approximated DF is

$$\begin{aligned} f(x:\alpha,\sigma,\mu) &\approx \frac{1}{2} \times \left(x^{-\alpha}\mathrm{e}^{\frac{1}{2}\alpha^2\sigma^2+\alpha\mu} \tanh\left(\frac{39\sqrt{2}\left(\alpha\sigma^2-\ln(x)+\mu\right)}{4\sigma\sqrt{\pi}} - \frac{111\arctan\left(\frac{35\sqrt{2}\left(\alpha\sigma^2-\ln(x)+\mu\right)}{222\sigma\sqrt{\pi}}\right)}{2} \right) \right. \\ &\left. - x^{-\alpha}\mathrm{e}^{\frac{1}{2}\alpha^2\sigma^2+\alpha\mu} - \tanh\left(-\frac{39\sqrt{2}\left(\ln(x)-\mu\right)}{4\sigma\sqrt{\pi}} + \frac{111\arctan\left(\frac{35\sqrt{2}\left(\ln(x)-\mu\right)}{222\sigma\sqrt{\pi}}\right)}{2} \right) + 1 \right), \end{aligned} \tag{22}$$

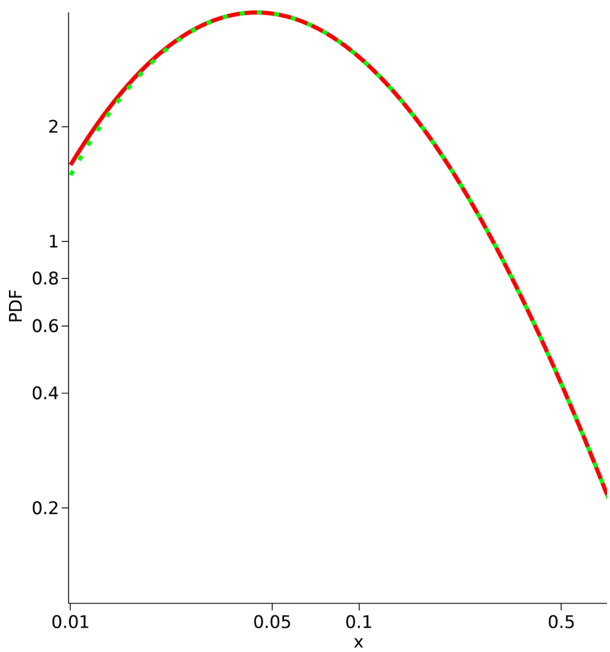

Figure 1. The modified lognormal with a power-law PDF with parameters $\mu = -2.04$, $\sigma = 1.044$ and $\alpha = 1.396$, red line, and approximated PDF, green points.

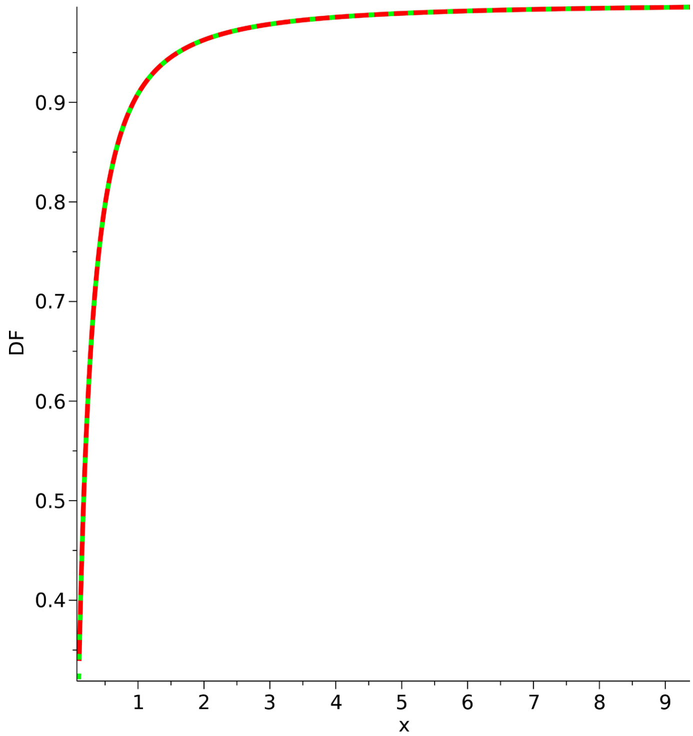

Figure 2. The modified lognormal with a power-law DF with parameters $\mu = -2.04$, $\sigma = 1.044$ and $\alpha = 1.396$, red line, and approximate DF, green points.

see **Figure 2**, which has a maximum percentage error of 0.05%.

The three parameters α, σ and μ can be obtained by two methods. The *first* method is via maximum likelihood (MLE), which maximizes

$$\Lambda = \frac{n\alpha^2\sigma^2}{2} + n\alpha\mu - n\ln(2) + n\ln(\alpha) + \sum_{j=1}^{n}\left(\ln\left(\operatorname{erfc}\left(\frac{\sqrt{2}\left(\alpha\sigma^2 - \ln(x_j) + \mu\right)}{2\sigma}\right)\right) - \ln(x_j)\alpha - \ln(x_j)\right), \tag{23}$$

where n is the number of elements in the sample x_j. This method was introduced by Fisher in 1921 and at the moment of writing is widely used. We extract the words used by Fisher "The solution of the problems of calculating from a sample the parameters of the hypothetical population, which we have put forward in the method of maximum likelihood, consists, then, simply of choosing such values of these parameters as have the maximum likelihood…" The derivatives of Λ with respect to α, σ and μ form a system of three nonlinear equations:

$$\frac{\partial\Lambda}{\partial\alpha} = n\alpha\sigma^2 + n\mu + \frac{n}{\alpha} + \sum_{j=1}^{n}\left(-\frac{e^{-\frac{\left(\alpha\sigma^2 - \ln(x_j) + \mu\right)^2}{2\sigma^2}}\sqrt{2}\sigma}{\sqrt{\pi}\operatorname{erfc}\left(\frac{\sqrt{2}\left(\alpha\sigma^2 - \ln(x_j) + \mu\right)}{2\sigma}\right)} - \ln(x_j)\right) = 0 \tag{24a}$$

$$\frac{\partial\Lambda}{\partial\mu}=n\alpha+\sum_{j=1}^{n}\left(-\frac{\mathrm{e}^{-\frac{\left(\alpha\sigma^2-\ln\left(x_j\right)+\mu\right)^2}{2\sigma^2}}\sqrt{2}}{\sqrt{\pi}\sigma\operatorname{erfc}\left(\frac{\sqrt{2}\left(\alpha\sigma^2-\ln\left(x_j\right)+\mu\right)}{2\sigma}\right)}\right)=0 \tag{24b}$$

$$\frac{\partial\Lambda}{\partial\sigma}=n\alpha^2\sigma+\sum_{j=1}^{n}\left(-\frac{2\mathrm{e}^{-\frac{\left(\alpha\sigma^2-\ln\left(x_j\right)+\mu\right)^2}{2\sigma^2}}\left(\sqrt{2}\alpha-\frac{\sqrt{2}\left(\alpha\sigma^2-\ln\left(x_j\right)+\mu\right)}{2\sigma^2}\right)}{\sqrt{\pi}\operatorname{erfc}\left(\frac{\sqrt{2}\left(\alpha\sigma^2-\ln\left(x_j\right)+\mu\right)}{2\sigma}\right)}\right)=0 \tag{24c}$$

which can be solved numerically. The *second* method minimizes the following χ^2

$$\chi^2=\sum_{i=1}^{n}\left(datadf_i-DF\left(x_i\right)\right)^2, \tag{25}$$

where the x_i are the elements of the sample sorted into ascending order, $datadf_i$ are the values of the empirical DF corresponding to x_i, see subroutine KSONE in [23], and $DF(x_i)$ are the theoretical values of the DF. This second method is classified as nonlinear least squares (NLLS). The derivatives of this χ^2 with respect to α, σ and μ form a system of three nonlinear equations:

$$\frac{\partial\chi^2}{\partial\alpha}=0 \tag{26a}$$

$$\frac{\partial\chi^2}{\partial\mu}=0 \tag{26b}$$

$$\frac{\partial\Lambda}{\partial\sigma}=0 \tag{26c}$$

which can be solved as non-linear least squares (NLLSQ). At the moment of writing, the above method is occasionally used in current research.

4. The Truncated MLP Distribution

The truncated version of the MLP defined in the interval $\left[x_l,x_u\right]$ has the following PDF:

$$f_T\left(x:\alpha,\sigma,\mu,x_l,x_u\right)=\frac{x^{-1-\alpha}\operatorname{erfc}\left(\frac{\sqrt{2}\left(\alpha\sigma-\frac{\ln(x)-\mu}{\sigma}\right)}{2}\right)}{A}, \tag{27}$$

where

$$A=\frac{1}{\alpha}\times\Bigg[\mathrm{e}^{-\frac{1}{2}\alpha^2\sigma^2-\alpha\mu}\operatorname{erf}\left(\frac{\sqrt{2}\left(\ln\left(x_u\right)-\mu\right)}{2\sigma}\right)
-\mathrm{e}^{-\frac{1}{2}\alpha^2\sigma^2-\alpha\mu}\operatorname{erf}\left(\frac{\sqrt{2}\left(\ln\left(x_l\right)-\mu\right)}{2\sigma}\right)
-x_l^{-\alpha}\operatorname{erf}\left(\frac{\sqrt{2}\left(\alpha\sigma^2-\ln\left(x_l\right)+\mu\right)}{2\sigma}\right)
+x_u^{-\alpha}\operatorname{erf}\left(\frac{\sqrt{2}\left(\alpha\sigma^2-\ln\left(x_u\right)+\mu\right)}{2\sigma}\right)+x_l^{-\alpha}-x_u^{-\alpha}\Bigg]. \tag{28}$$

The DF is

$$F_T\left(x:\alpha,\sigma,\mu,x_l,x_u\right)=\frac{1}{\alpha A}\times\Bigg[-x_l^{-\alpha}\operatorname{erf}\left(\frac{\sqrt{2}\left(\alpha\sigma^2-\ln\left(x_l\right)+\mu\right)}{2\sigma}\right)
+\mathrm{e}^{-\frac{1}{2}\alpha^2\sigma^2-\alpha\mu}\operatorname{erf}\left(\frac{\sqrt{2}\left(\ln\left(x\right)-\mu\right)}{2\sigma}\right)
-\mathrm{e}^{-\frac{1}{2}\alpha^2\sigma^2-\alpha\mu}\operatorname{erf}\left(\frac{\sqrt{2}\left(\ln\left(x_l\right)-\mu\right)}{2\sigma}\right)
+x^{-\alpha}\operatorname{erf}\left(\frac{\sqrt{2}\left(\alpha\sigma^2-\ln\left(x\right)+\mu\right)}{2\sigma}\right)-x^{-\alpha}+x_l^{-\alpha}\Bigg]. \tag{29}$$

The first moment or average value is

$$E\left(x:\alpha,\sigma,\mu,x_l,x_u\right)
=\frac{1}{A\left(-1+\alpha\right)}\times\Bigg[\mathrm{e}^{-\frac{1}{2}\alpha^2\sigma^2-\alpha\mu+\frac{1}{2}\sigma^2+\mu}\operatorname{erf}\left(\frac{\sqrt{2}\left(\sigma^2-\ln\left(x_l\right)+\mu\right)}{2\sigma}\right)
-\mathrm{e}^{-\frac{1}{2}\alpha^2\sigma^2-\alpha\mu+\frac{1}{2}\sigma^2+\mu}\operatorname{erf}\left(\frac{\sqrt{2}\left(\sigma^2-\ln\left(x_u\right)+\mu\right)}{2\sigma}\right)
-x_l^{1-\alpha}\operatorname{erf}\left(\frac{\sqrt{2}\left(\alpha\sigma^2-\ln\left(x_l\right)+\mu\right)}{2\sigma}\right)
+x_u^{1-\alpha}\operatorname{erf}\left(\frac{\sqrt{2}\left(\alpha\sigma^2-\ln\left(x_u\right)+\mu\right)}{2\sigma}\right)+x_l^{1-\alpha}-x_u^{1-\alpha}\Bigg], \tag{30}$$

and the second moment is

$$E\left(x^2:\alpha,\sigma,\mu,x_l,x_u\right)
=\frac{1}{A\left(-2+\alpha\right)}\times\Bigg[\mathrm{e}^{-\left(-2+\alpha\right)\left(\frac{1}{2}\alpha\sigma^2+\sigma^2+\mu\right)}\operatorname{erf}\left(\frac{\sqrt{2}\left(-2\sigma^2+\ln\left(x_u\right)-\mu\right)}{2\sigma}\right)
-\mathrm{e}^{-\left(-2+\alpha\right)\left(\frac{1}{2}\alpha\sigma^2+\sigma^2+\mu\right)}\operatorname{erf}\left(\frac{\sqrt{2}\left(-2\sigma^2+\ln\left(x_l\right)-\mu\right)}{2\sigma}\right)$$

$$-x_l^{2-\alpha}\,\mathrm{erf}\left(\frac{\sqrt{2}\left(\alpha\sigma^2-\ln\left(x_l\right)+\mu\right)}{2\sigma}\right)$$
$$\left.+x_u^{2-\alpha}\,\mathrm{erf}\left(\frac{\sqrt{2}\left(\alpha\sigma^2-\ln\left(x_u\right)+\mu\right)}{2\sigma}\right)+x_l^{2-\alpha}-x_u^{2-\alpha}\right]. \tag{31}$$

The variance, in an implicit form, is

$$Var\left(\alpha,\sigma,\mu,x_l,x_u\right)=E\left(x^2:\alpha,\sigma,\mu,x_l,x_u\right)-\left(E\left(x:\alpha,\sigma,\mu,x_l,x_u\right)\right)^2. \tag{32}$$

The *first* method to derive the three basic parameters is the maximum likelihood (MLE), which maximizes

$$\Lambda=n\ln\left(-\frac{1}{\left(B-C\right)\mathrm{e}^{-\frac{1}{2}\alpha^2\sigma^2-\alpha\mu}+\left(D-1\right)x_l^{-\alpha}-x_u^{-\alpha}\left(E-1\right)}\right)+n\ln\left(\alpha\right)$$
$$+\sum_{j=1}^{n}\left(-\ln\left(x_j\right)\alpha-\ln\left(x_j\right)+\ln\left(\mathrm{erfc}\left(\frac{\sqrt{2}\left(\alpha\sigma^2-\ln\left(x_j\right)+\mu\right)}{2\sigma}\right)\right)\right), \tag{33}$$

where

$$B=\mathrm{erf}\left(\frac{\sqrt{2}\left(\ln\left(x_l\right)-\mu\right)}{2\sigma}\right), \tag{34a}$$

$$C=\mathrm{erf}\left(\frac{\sqrt{2}\left(\ln\left(x_u\right)-\mu\right)}{2\sigma}\right), \tag{34b}$$

$$D=\mathrm{erf}\left(\frac{\sqrt{2}\left(\alpha\sigma^2-\ln\left(x_l\right)+\mu\right)}{2\sigma}\right), \tag{34c}$$

$$E=\mathrm{erf}\left(\frac{\sqrt{2}\left(\alpha\sigma^2-\ln\left(x_u\right)+\mu\right)}{2\sigma}\right). \tag{34d}$$

where n is the number of elements of the sample x_j and x_l and x_u are respectively the minimum and maximum of the sample x_j. The derivatives of Λ with respect to α, σ and μ form a system of three nonlinear equations here given in implicit form:

$$\frac{\partial\Lambda\left(\alpha,\sigma,\mu,x_l,x_u\right)}{\partial\alpha}=0, \tag{35a}$$

$$\frac{\partial\Lambda\left(\alpha,\sigma,\mu,x_l,x_u\right)}{\partial\mu}=0, \tag{35b}$$

$$\frac{\partial\Lambda\left(\alpha,\sigma,\mu,x_l,x_u\right)}{\partial\sigma}=0, \tag{35c}$$

which can be solved numerically. The second method implements the NLLSQ method, see Equation (25), for the truncated MLP distribution.

The Average Value

An application of the above formulae is the behaviour of the truncated average value as a function of the upper limit for the mass of the stars, $\mathcal{M}_\odot$, here identified with the random variable X. The average value of the mass in the MLP distribution as given by Formula (30) with parameters $\mu = -2.04$, $\sigma = 1.044$ and $\alpha = 1.396$ is $E(\mathcal{M}_\odot) = 0.549\mathcal{M}_\odot$. The average value of the mass for the truncated MLP distribution as given by Formula (30) is shown in **Figure 3**. It is interesting to observe that at $x_u = 80\mathcal{M}_\odot$ the average value is 0.489.

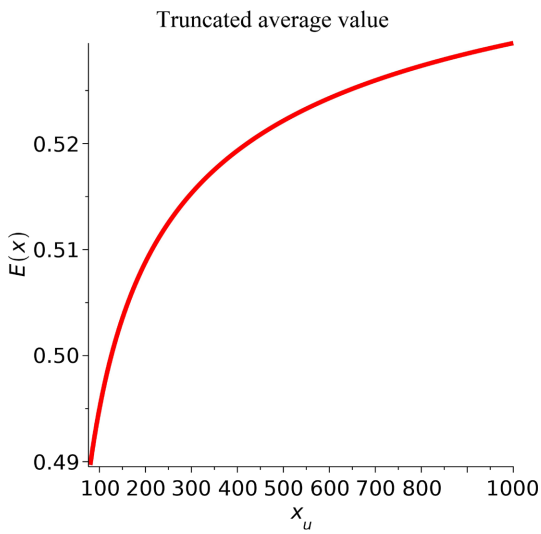

Figure 3. The behavior of the average value for the truncated MLP distribution as a function of the upper limit of the mass with parameters $x_l = 0.01$, $\mu = -2.04$, $\sigma = 1.044$ and $\alpha = 1.396$.

5. Astrophysical Applications

We now introduce these distributions and analyse five clusters of stars and one cluster of galaxies.

5.1. Adopted Statistics

The Kolmogorov-Smirnov test (K-S), see [24]-[26], does not require the data to be binned. The K-S test, as implemented by the FORTRAN subroutine KSONE in [23], finds the maximum distance, D, between the theoretical and the astronomical DFs, as well as the significance level P_{KS}; see formulas 14.3.5 and 14.3.9 in [23]. If $P_{KS} \geq 0.1$, then the goodness of the fit is believable.

5.2. The Mass Distribution for Clusters of Stars

The *first* test is performed on NGC 2362, where the masses of the 271 stars have a range of $1.47M_\odot \geq M \geq 0.11M_\odot$, see [27] and CDS catalog J/MNRAS/384/675/**Table1**. The *second* test is performed on the low-mass stars in the young cluster NGC 6611, see [28] and CDS catalog J/MNRAS/392/1034. This massive cluster has an age of 2 - 3 Myr and contains masses from

$1.5M_{\odot} \geq M \geq 0.02M_{\odot}$. Therefore, the brown dwarfs (BD) region, $\approx 0.2\mathcal{M}_{\odot}$, is covered. The *third* test is performed on the γ Velorum cluster, where the 237 stars have a range of $1.31M_{\odot} \geq M \geq 0.15M_{\odot}$, see [29] and CDS catalog J/A + A/589/A70/Table 5. The *fourth* test is performed on the young cluster Berkeley 59, where the 420 stars have a range of $2.24M_{\odot} \geq M \geq 0.15M_{\odot}$, see [30] and CDS catalog J/AJ/155/44/Table 3. The fifth test is performed on the Hyades, where the 602 stars have a range of $2.20M_{\odot} \geq M \geq 0.11M_{\odot}$, see [31] and CDS catalog J/AJ/165/108/Table 1. The statistics for the lognormal distribution for these five astronomical samples of stars are given in Table 1, for the truncated lognormal distribution in Table 2, for the double Pareto-lognormal distribution in Table 3, for the MLP distribution in Table 4 and for the MLP distribution in Table 5.

Table 1. Numerical values of D, the maximum distance between theoretical and observed DFs, and P_{KS}, significance level, in the K-S test for the lognormal distribution, see Equation (4), for different mass distributions.

Cluster	Parameters	D	P_{KS}
NGC 2362	$\sigma = 0.5$, $\mu = -0.55$	0.073	0.105
NGC 6611	$\sigma = 1.03$, $\mu = -1.26$	0.093	0.049
γ Velorum	$\sigma = 0.5$, $\mu = -1.08$	0.092	0.033
Berkeley 59	$\sigma = 0.49$, $\mu = -0.92$	0.11	6.46×10^{-5}
Hyades	$\sigma = 0.69$, $\mu = -0.91$	0.065	0.01

Table 2. Numerical values of D, the maximum distance between theoretical and observed DFs, and P_{KS}, significance level, in the K-S test for the truncated lognormal distribution, see Equation (8), for different mass distributions.

Cluster	Parameters	D	P_{KS}
NGC 2362	$\sigma = 0.59$, $\mu = -0.47$	0.047	0.556
NGC 6611	$\sigma = 1.49$, $\mu = -0.73$	0.065	0.32
γ Velorum	$\sigma = 0.8$, $\mu = -1.47$	0.052	0.50
Berkeley 59	$\sigma = 0.56$, $\mu = -0.99$	0.086	2.51×10^{-3}
Hyades	$\sigma = 0.89$, $\mu = -1.06$	0.035	0.42

Table 3. Numerical values of D, the maximum distance between theoretical and observed DFs, and P_{KS}, significance level, in the K-S test for the double Pareto-lognormal distribution see Equation (12), for different mass distributions.

Cluster	Parameters	D	P_{KS}
NGC 2362	$\alpha = 7.61$, $\beta = 5.46$, $\sigma = 0.449$, $\mu = -0.498$	0.0685	0.148
NGC 6611	$\alpha = 5.04$, $\beta = 5.51$, $\sigma = 0.99$, $\mu = -1.27$	0.0935	0.05

Continued

γ Velorum	$\alpha = 8.52$, $\beta = 9.73$, $\sigma = 0.47$, $\mu = -1.1$	0.091	0.037
Berkeley 59	$\alpha = 11.16$, $\beta = 8.65$, $\sigma = 0.47$, $\mu = -0.9$	0.11	7×10^{-5}
Hyades	$\alpha = 4.4$, $\beta = 6.67$, $\sigma = 0.63$, $\mu = -0.99$	0.064	0.01

Table 4. Adopted method to derive the parameters, numerical values of D, the maximum distance between theoretical and observed DFs, and P_{KS}, significance level, in the K-S test for the MLP distribution, see Equation (15), for different mass distributions.

Cluster	Method	Parameters	D	P_{KS}
NGC 2362	NLLS	$\sigma = 0.46$, $\mu = -0.8$, $\alpha = 3.34$	0.082	0.046
NGC 6611	MLE	$\sigma = 1$, $\mu = -1.62$, $\alpha = 3.52$	0.08	0.127
γ Velorum	NLLS	$\sigma = 0.22$, $\mu = -1.62$, $\alpha = 1.76$	0.037	0.89
Berkeley 59	MLE	$\sigma = 0.18$, $\mu = -1.41$, $\alpha = 2.01$	0.036	0.63
Hyades	MLE	$\sigma = 0.57$, $\mu = -1.32$, $\alpha = 2.47$	0.054	0.053

Table 5. Adopted method to derive the parameters, numerical values of D, the maximum distance between theoretical and observed DFs, and P_{KS}, significance level, in the K-S test for the truncated MLP distribution, see Equation (31), for different mass distributions.

Cluster	Method	Parameters	D	P_{KS}
NGC 2362	MLE	$\sigma = 0.56$, $\mu = -0.71$, $\alpha = 3.7$	0.051	0.45
NGC 6611	NLLS	$\sigma = 1.4$, $\mu = -1.01$, $\alpha = 3.35$	0.06	0.358
γ Velorum	NLLS	$\sigma = 0.66$, $\mu = -1.47$, $\alpha = 9.17$	0.0521	0.53

Continued

Berkeley 59	MLE	$\sigma = 0.17$, $\mu = -1.43$, $\alpha = 1.78$	0.032	0.76
Hyades	MLE	$\sigma = 0.82$, $\mu = -1.36$, $\alpha = 3.02$	0.035	0.43

As an example, the empirical PDF visualized through histograms and the PDF of the theoretical truncated MLP for the NGC 2362 cluster are presented in Figure 4, the results for the cluster NGC 6611 are presented in Figure 5 and those for the γ Velorum cluster in Figure 6. The empirical DF and the theoretical truncated MLP for the cluster Berkeley 59 are presented in Figure 7, and those for the Hyades are presented in Figure 8.

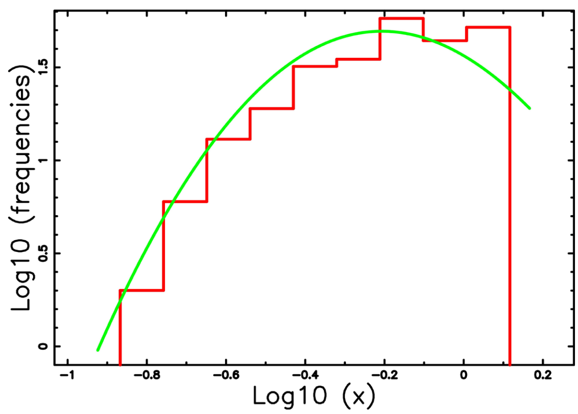

Figure 4. Logarithmic histogram of mass distribution as given by NGC 2362 cluster data (red) with a superposition of the truncated MLP distribution when the number of bins, m, is 10 (green line). Parameters as in Table 5. Vertical and horizontal axes have logarithmic scales.

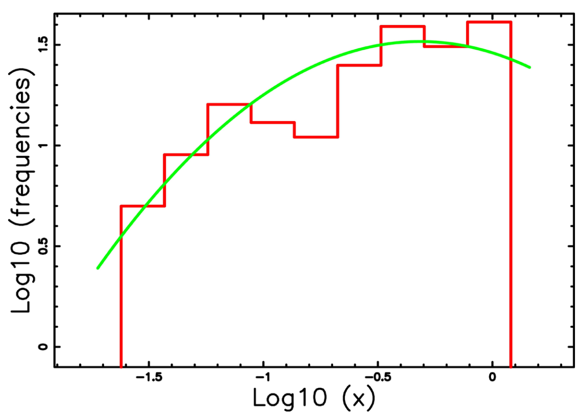

Figure 5. Logarithmic histogram of mass distribution as given by NGC 6611 cluster data (red) with a superposition of the left truncated MLP distribution when the number of bins, m, is 10 (green line). Parameters as in Table 5. Vertical and horizontal axes have logarithmic scales.

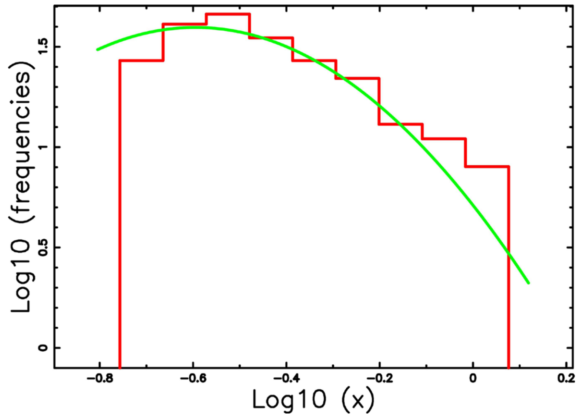

Figure 6. Logarithmic histogram of mass distribution as given by γ Velorum cluster data (red) with a superposition of the truncated MLP distribution when the number of bins, m, is 10 (green line). Parameters as in Table 5. Vertical and horizontal axes have logarithmic scales.

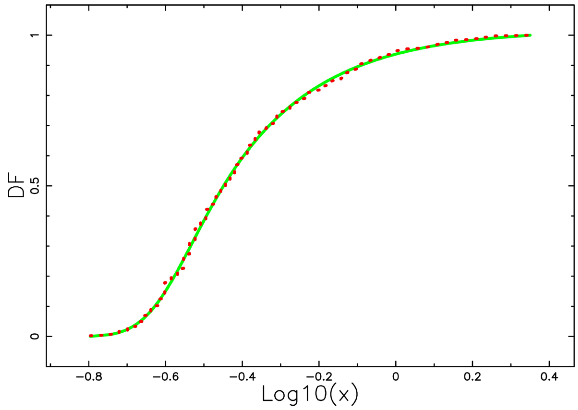

Figure 7. DF of mass distribution as given by Berkeley 59 cluster data (red points) with a superposition of the truncated MLP distribution when the number of bins, m, is 10 (green line). Parameters as in Table 5. The horizontal axis has a logarithmic scale.

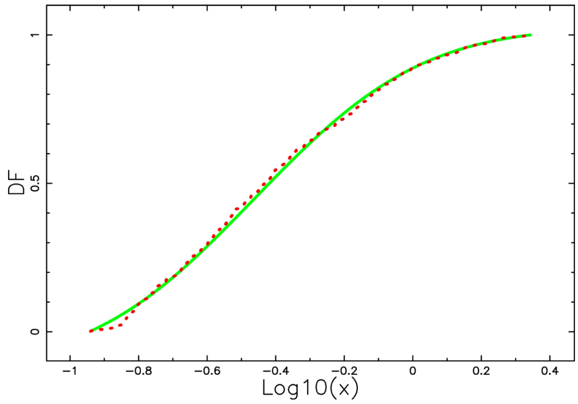

Figure 8. DF of mass distribution as given by Hyades cluster data (red points) with a superposition of the truncated MLP distribution when the number of bins, m, is 10 (green line). Parameters as in Table 5. The horizontal axis has a logarithmic scale.

5.3. The Mass Distribution of Galaxies

We tested a sample for the total HI mass (MHI) of 175 galaxies, which is also available at CDS [32]. The mass of the galaxies as given by the catalog is expressed in $10^9 \mathcal{M}_\odot$, for further comparison with the stars we expressed the mass in in $10^{10} \mathcal{M}_\odot$. The empirical PDF for the galaxies' mass is visualized through histograms and the PDF of the theoretical truncated MLP is presented in Figure 9. The parameters for the distributions used here are given in Table 6.

Table 6. Numerical values of D, the maximum distance between theoretical and observed DFs, and P_{KS}, significance level, in the K-S test for the lognormal distribution, for the mass of the galaxies expressed in $10G\mathcal{M}_\odot$.

Distribution	Parameters	D	P_{KS}
Lognormal	$\sigma=1.62$, $\mu=-1.83$	0.046	0.841
Truncated lognormal	$\sigma=1.81$, $\mu=-1.66$	0.0541	0.671
Double pareto-lognormal	$\alpha=4.49$, $\beta=4.57$, $\sigma=1.59$, $\mu=-1.8$	0.264	3×10^{-11}
MLP	$\sigma=1.49$, $\mu=-2.07$, $\alpha=3.31$	0.0318	0.99
Truncated MLP	$\sigma=1.72$, $\mu=-2.29$, $\alpha=1.51$,	0.0535	0.685

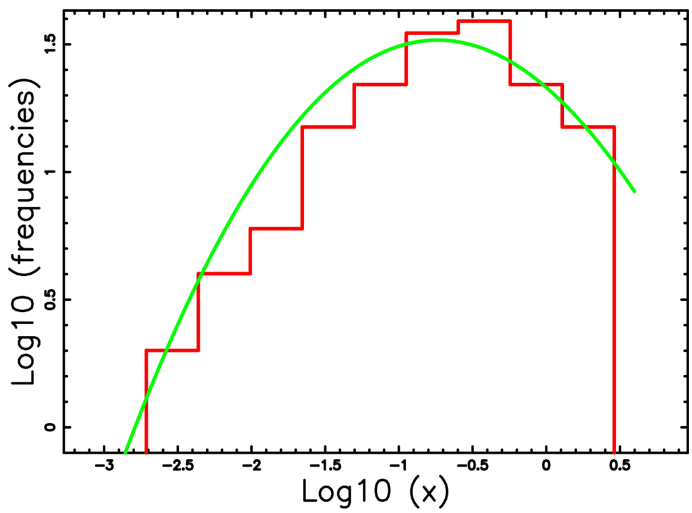

Figure 9. Logarithmic histogram of mass distribution for galaxies (red) with a superposition of the truncated MLP distribution when the number of bins, m, is 10 (green line). Parameters as in Table 6. Vertical and horizontal axes have logarithmic scales.

6. The Initial Mass Function for Stars

In the following, m is the stellar mass in units of $\mathcal{M}_\odot$. The *first* model for the initial mass function (IMF) is given by three power laws of the type

$$p_{stars}(m) \propto m^{-\alpha_i}, \tag{36}$$

each zone being characterized by a different exponent α_i. In order to have a PDF normalized to unity, one must have

$$\sum_{i=1,3}\int_{m_i}^{m_{i+1}} c_i m^{-\alpha_i}\mathrm{d}m = 1. \tag{37}$$

For example, we start with $c_1 = 1$: c_2 will be determined by the following equation

$$c_1\left(0.5-\epsilon\right)^{-\alpha_1} = c_2\left(0.5+\epsilon\right)^{-\alpha_2}, \tag{38}$$

where ϵ is a small number, e.g. $\epsilon = 10^{-4}$. In the previous equation we insert $\alpha_1 = 1.3$ and $\alpha_2 = 2.3$ and therefore $c_2 = 0.503$. The same procedure applied for c_3 gives $c_3 = 0.506$. The integral of $p_{stars}(m)$ over the field of existence now gives 4.14, but according to the requirement of normalization as given by Equation (37), it should be 1. As a consequence, the three constants are now $c_1 = 0.24$, $c_2 = 0.1205$, and $c_3 = 0.1206$, which is the same as Equation (59) in [33]

$$p(m) = \begin{cases} \dfrac{0.1206}{m^{2.7}} & 1.0 \le m \\ \dfrac{0.1205}{m^{2.3}} & 0.50 \le m \\ \dfrac{0.2409}{m^{1.3}} & 0.07 \le m \\ 0 & 10.0 < m \end{cases}. \tag{39}$$

The mean of the galactic IMF is given by a numerical integration over the three zones

$$\overline{m} = \sum_{i=1,3}\int_{m_i}^{m_{i+1}} c_i m m^{-\alpha_i}\mathrm{d}m = 0.389. \tag{40}$$

The presence of the brown dwarfs means the use of four power laws instead of three power laws:

$$p(m) = \begin{cases} \dfrac{0.07675}{m^{2.7}} & 1.0 \le m \\ \dfrac{0.0767}{m^{2.3}} & 0.50 \le m \\ \dfrac{0.1535}{m^{1.3}} & 0.07 \le m \\ \dfrac{2.1928}{m^{0.3}} & 0.01 \le m \\ 0 & 100.0 \le m \end{cases}, \tag{41}$$

where in order to have a continuous PDF, the BDs have the range $0.01 < m \le 0.07$ rather than $0.01 < m \le 0.15$, see Equation (59) in [33]. The mean of the galactic IMF with four power laws is 0.2788. More details on this *first* model can be found in [34]. The *second* model for the IMF is due to Chabrier 2005, more precisely formula (1) in [35], which is here presented as a PDF in a normalized form

$$\xi(m) = \frac{3.3799\left(\begin{cases} 0.093\mathrm{e}^{-1.6528\left(\frac{\ln(m)}{\ln(10)}+0.6989700043\right)^2} & m < 1 \\ \frac{0.0414}{m^{1.35}} & m < \infty \end{cases}\right)}{m}. \quad (42)$$

The average value for Chabrier's PDF is 0.623. Astronomers usually report the data on the IMF in logarithmic bins and therefore the IMF is

$$\frac{\mathrm{d}N}{\mathrm{d}\log(m)} = mf(m), \quad (43)$$

where $f(m)$ is the considered normalized PDF and the two IMFs are given in Figure 10.

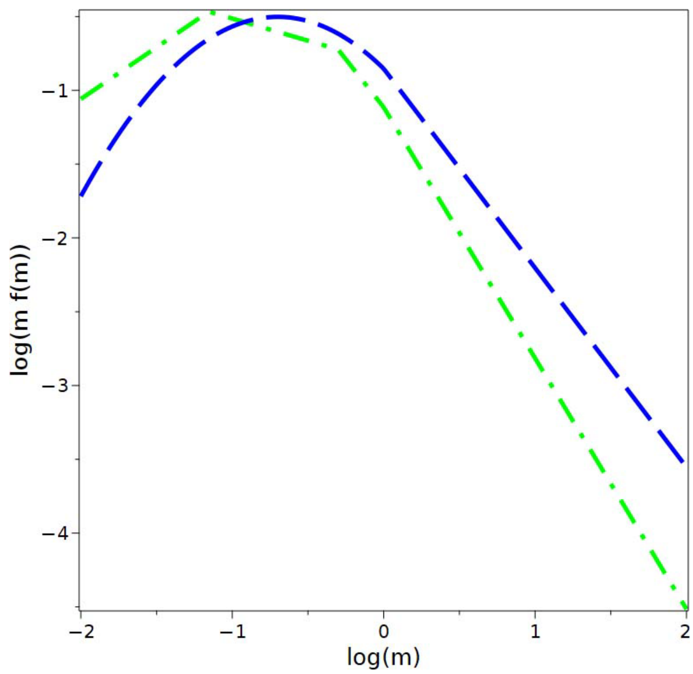

Figure 10. Comparison of the IMF of Chabrier 2005, blue dashed line, with the IMF of Kroupa 2012, green dash-dot line.

The comparison between the IMF of Chabrier 2005 and the MLP IMF has already been done by [20], obtaining the set of parameters $\mu = -2.04$, $\sigma = 1.044$ and $\alpha = 1.396$. We therefore evaluated the parameters of the best fit between Chabrier 2005 and truncated MLP, obtaining $\mu = -2.34$, $\sigma = 1.086$ and $\alpha = 1.406$ when the lower boundary for $\log(m)$ is −2 and the upper 2, see Figure 11.

7. Conclusions

The truncated MLP

We derived the PDF, the DF, the average value, the second moment, using the MLE and NLLSQ methods to extract the parameters for the truncated MLP distribution.

Fitting single clusters of stars

Table 7 presents the best distribution for the five catalogs used here. The truncated MLP yields the best result in three clusters over the five analysed.

Table 7. The best fitting distribution and P_{KS}, significance level, in the K-S test, for different mass distributions.

Cluster	Distribution	P_{KS}
NGC 2362	Truncated lognormal	0.556
NGC 6611	Truncated MLP	0.358
γ Velorum	MLP	0.89
Berkeley 59	Truncated MLP	0.76
Hyades	Truncated MLP	0.43

The results for the mass distribution of the γ Velorum cluster compared with other distributions are shown in Table 8, in which the truncated MLP distribution occupies the first position together with the Benini distribution.

Table 8. Numerical values of D, the maximum distance between the theoretical and observed DFs, and P_{KS}, the significance level, in the K-S test for different distributions in the case of γ Velorum cluster.

Distribution	Reference	D	P_{KS}
MLP	here	0.037	0.89
MLP truncated	here	0.052	0.53
Benini	[36]	0.0372	0.89
Benini right truncated	[36]	0.042	0.779
Truncated gompertz	[37]	0.173	9.27×10^{-7}
Truncated topp-leone	[38]	6.09×10^{-2}	0.25
Frèchet	[39]	0.125	3.13×10^{-4}
Truncated Frèchet	[39]	0.077	0.07
Truncated Weibull	[40]	0.046	0.576
Truncated Sujatha	[41]	0.0485	0.534
Truncated Lindley	[42]	0.11	0.48
Generalized gamma	[5]	0.11	1.24×10^{-3}
Truncated generalized gamma	[5]	0.062	0.24
Lognormal	[18]	0.0729	0.11
Truncated lognormal	[18]	0.047	0.55
Gamma	[43]	0.059	0.28
Truncated gamma	[43]	0.0754	0.08
Beta	[34]	0.059	0.28

A careful reading of the above table allows us to conclude that when the range in mass analysed covers $\approx$ one decade, other distributions, such as the Benini, are competitive with the lognormal family.

Mass function

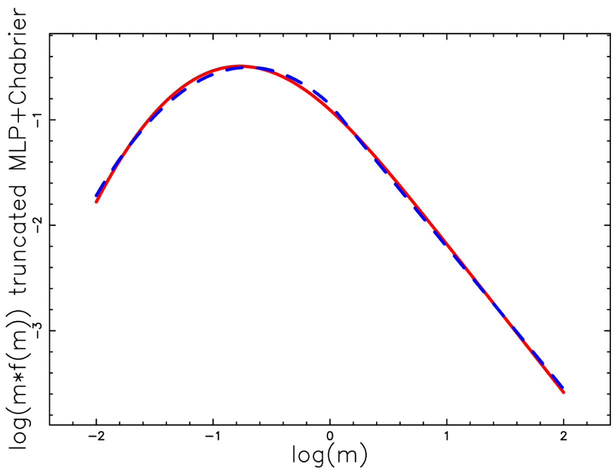

Figure 11. Comparison of the IMF of Chabrier 2005, blue dashed line, with the truncated MLP IMF, red line.

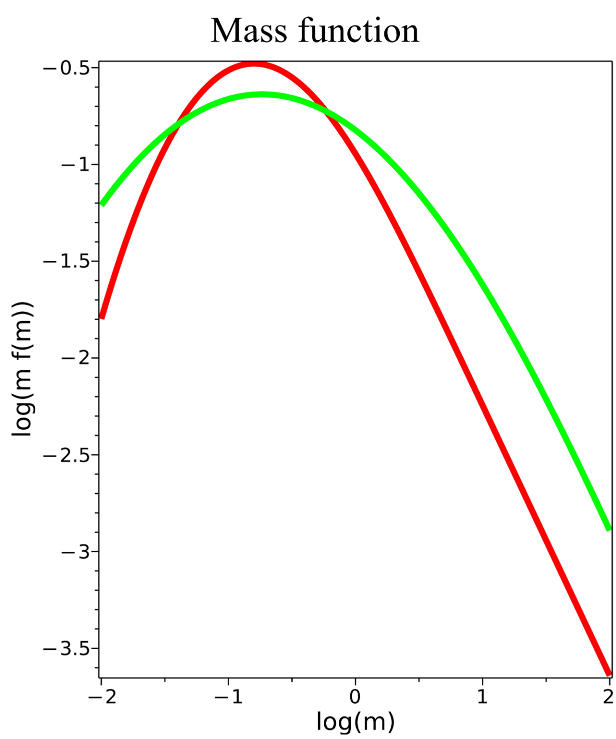

Figure 12. Display of the truncated MLP MF for stars (red line) with parameters as in Figure 11 and the truncated MLP MF for galaxies (green line) with parameters as in Table 6.

We have fitted the data of the IMF for stars with the truncated MLP function and the results are presented in Figure 11. Now, the insertion of a lower and an upper logarithm of the mass has a theoretical explanation. In other words, the basic question (2) in the introduction has now been answered. The analogy between the scaling of the mass of the stars and that of the galaxies, as shown in **Figure 12**, is interesting. The above figure points toward a similar mechanism of formation for stars and galaxies.

Conflicts of Interest

The author declares no conflicts of interest regarding the publication of this paper.

References

[1] Pearson, K. (1902) V. on the Methematical Theory of Errors of Judgement, with Special Reference to the Personal Equation. *Philosophical Transactions of the Royal Society of London. Series A, Containing Papers of a Mathematical or Physical Character*, **198**, 235-299.

[2] Zaninetti, L. (2022) New Probability Distributions in Astrophysics: IX. Truncation for Exponential, Half Gaussian and Sech-Square Distributions with Application to the Galactic Height. *International Journal of Astronomy and Astrophysics*, **12**, 328-346. https://doi.org/10.4236/ijaa.2022.124019

[3] Schechter, P. (1976) An Analytic Expression for the Luminosity Function for Galaxies. *The Astrophysical Journal*, **203**, 297-306. https://doi.org/10.1086/154079

[4] Zaninetti, L. (2010) The Luminosity Function of Galaxies as Modelled by the Generalized Gamma Distribution. *Acta Physica Polonica B*, **41**, 729-751.

[5] Zaninetti, L. (2019) New Probability Distributions in Astrophysics: I. The Truncated Generalized Gamma. *International Journal of Astronomy and Astrophysics*, **9**, 393-410. https://doi.org/10.4236/ijaa.2019.94027

[6] Galton, F. (1879) XII. The Geometric Mean, in Vital and Social Statistics. *Proceedings of the Royal Society of London*, **29**, 365-367.

[7] McAlister, D. (1879) XIII. The Law of the Geometric Mean. *Proceedings of the Royal Society of London*, **29**, 367-376.

[8] Cobb, C.W. and Douglas, P.H. (1928) A Theory of Production. *American Economic Association*, **18**, 139-165.

[9] Gibrat, R. (1931) Les Inégalites Économiques. Sirey.

[10] Nydell, S. (1919) The Mean Errors of the Characteristics in Logarithmic-Normal Distributions. *Scandinavian Actuarial Journal*, **1919**, 134-144. https://doi.org/10.1080/03461238.1919.10414805

[11] Scargle, J.D. (2020) Studies in Astronomical Time-Series Analysis. VII. An Enquiry Concerning Nonlinearity, the Rms-Mean Flux Relation, and Lognormal Flux Distributions. *The Astrophysical Journal*, **895**, Article 90. https://doi.org/10.3847/1538-4357/ab8d38

[12] Shah, Z., Misra, R. and Sinha, A. (2020) On the Determination of Lognormal Flux Distributions for Astrophysical Systems. *Monthly Notices of the Royal Astronomical Society*, **496**, 3348-3357. https://doi.org/10.1093/mnras/staa1746

[13] Banda-Barragán, W.E., Brüggen, M., Federrath, C., Wagner, A.Y., Scannapieco, E. and Cottle, J. (2020) Shock-Multicloud Interactions in Galactic Outflows—I. Cloud Layers with Lognormal Density Distributions. *Monthly Notices of the Royal Astronomical Society*, **499**, 2173-2195. https://doi.org/10.1093/mnras/staa2904

[14] Nagovitsyn, Y.A. and Pevtsov, A.A. (2021) Bi-Lognormal Distribution of Sunspot Group Areas. *The Astrophysical Journal*, **906**, Article 27. https://doi.org/10.3847/1538-4357/abc82d

[15] Wang, N., Yi, T., Wang, L., Mao, L., Pu, Z., Ning, G., *et al.* (2023) Comprehensive Study of the Blazars from Fermi-Lat LCR: The Log-Normal Flux Distribution and Linear Rms-Flux Relation. *Research in Astronomy and Astrophysics*, **23**, Article 115011. https://doi.org/10.1088/1674-4527/ace9b1

[16] Evans, M., Hastings, N. and Peacock, B. (2000) Statistical Distributions. 3rd Edition, John Wiley & Sons Inc.

[17] Johnson, N.L., Kotz, S. and Balakrishnan, N. (1994) Continuous Univariate Distributions. Vol. 1. 2nd Edition, Wiley.

[18] Zaninetti, L. (2017) A Left and Right Truncated Lognormal Distribution for the Stars. *Advances in Astrophysics*, **2**, 197-213. https://doi.org/10.22606/adap.2017.23005

[19] Reed, W.J. and Jorgensen, M. (2004) The Double Pareto-Lognormal Distribution—A New Parametric Model for Size Distributions. *Communications in Statistics-Theory and Methods*, **33**, 1733-1753. https://doi.org/10.1081/sta-120037438

[20] Basu, S., Gil, M. and Auddy, S. (2015) The MLP Distribution: A Modified Lognormal Power-Law Model for the Stellar Initial Mass Function. *Monthly Notices of the Royal Astronomical Society*, **449**, 2413-2420. https://doi.org/10.1093/mnras/stv445

[21] Howard, R.M. (2022) Arbitrarily Accurate Analytical Approximations for the Error Function. *Mathematical and Computational Applications*, **27**, Article 14. https://doi.org/10.3390/mca27010014

[22] Vazquez-Leal, H., Castaneda-Sheissa, R., Filobello-Nino, U., Sarmiento-Reyes, A. and Sanchez Orea, J. (2012) High Accurate Simple Approximation of Normal Distribution Integral. *Mathematical Problems in Engineering*, **2012**, Article ID: 124029. https://doi.org/10.1155/2012/124029

[23] Press, W.H., Teukolsky, S.A., Vetterling, W.T. and Flannery, B.P. (1992) Numerical Recipes in FORTRAN. The Art of Scientific Computing. Cambridge University Press.

[24] Kolmogoroff, A. (1941) Confidence Limits for an Unknown Distribution Function. *The Annals of Mathematical Statistics*, **12**, 461-463. https://doi.org/10.1214/aoms/1177731684

[25] Smirnov, N. (1948) Table for Estimating the Goodness of Fit of Empirical Distributions. *The Annals of Mathematical Statistics*, **19**, 279-281. https://doi.org/10.1214/aoms/1177730256

[26] Massey, F.J. (1951) The Kolmogorov-Smirnov Test for Goodness of Fit. *Journal of the American Statistical Association*, **46**, 68-78. https://doi.org/10.2307/2280095

[27] Irwin, J., Hodgkin, S., Aigrain, S., Bouvier, J., Hebb, L., Irwin, M., *et al.* (2008) The Monitor Project: Rotation of Low-Mass Stars in NGC 2362—Testing the Disc Regulation Paradigm at 5 Myr. *Monthly Notices of the Royal Astronomical Society*, **384**, 675-686. https://doi.org/10.1111/j.1365-2966.2007.12725.x

[28] Oliveira, J.M., Jeffries, R.D. and van Loon, J.T. (2009) The Low-Mass Initial Mass Function in the Young Cluster NGC 6611. *Monthly Notices of the Royal Astronomical Society*, **392**, 1034-1050. https://doi.org/10.1111/j.1365-2966.2008.14140.x

[29] Prisinzano, L., Damiani, F., Micela, G., Jeffries, R.D., Franciosini, E., Sacco, G.G., *et al.* (2016) The *Gaia*-ESO Survey: Membership and Initial Mass Function of The γ Velorum Cluster. *Astronomy & Astrophysics*, **589**, A70. https://doi.org/10.1051/0004-6361/201527875

[30] Panwar, N., Pandey, A.K., Samal, M.R., Battinelli, P., Ogura, K., Ojha, D.K., *et al.* (2018) Young Cluster Berkeley 59: Properties, Evolution, and Star Formation. *The Astronomical Journal*, **155**, Article 44. https://doi.org/10.3847/1538-3881/aa9f1b

[31] Brandner, W., Calissendorff, P. and Kopytova, T. (2023) Astrophysical Properties of 600 Bona Fide Single Stars in the Hyades Open Cluster. *The Astronomical Journal*, **165**, Article 108. https://doi.org/10.3847/1538-3881/acb208

[32] Lelli, F., McGaugh, S.S. and Schombert, J.M. (2016) SPARC: Mass Models for 175 Disk Galaxies with Spitzer Photometry and Accurate Rotation Curves. *The Astronomical Journal*, **152**, Article 157. https://doi.org/10.3847/0004-6256/152/6/157

[33] Kroupa, P., Weidner, C., Pflamm-Altenburg, J., Thies, I., Dabringhausen, J., Marks, M., *et al.* (2013) The Stellar and Sub-Stellar Initial Mass Function of Simple and Composite Populations. In: Oswalt, T.D. and Gilmore, G., Eds., *Planets*, *Stars and Stellar Systems*, Springer, 115-242. https://doi.org/10.1007/978-94-007-5612-0_4

[34] Zaninetti, L. (2013) The Initial Mass Function Modeled by a Left Truncated Beta Distribution. *The Astrophysical Journal*, **765**, Article 128. https://doi.org/10.1088/0004-637x/765/2/128

[35] Chabrier, G. (2005) The Initial Mass Function: From Salpeter 1955 to 2005. In: Corbelli, E., Palla, F., Zinnecker, H. Eds., *The Initial Mass Function 50 Years Later*, Springer, 41-50. https://doi.org/10.1007/978-1-4020-3407-7_5

[36] Zaninetti, L. (2024) New Probability Distributions in Astrophysics: XIII. Truncation for the Benini Distribution. *International Journal of Astronomy and Astrophysics*, **14**, 203-219. https://doi.org/10.4236/ijaa.2024.143013

[37] Zaninetti, L. (2024) New Probability Distributions in Astrophysics: XII. Truncation for the Gompertz Distribution. *International Journal of Astronomy and Astrophysics*, **14**, 101-119. https://doi.org/10.4236/ijaa.2024.142007

[38] Zaninetti, L. (2023) New Probability Distributions in Astrophysics: XI. Left Truncation for the Topp-Leone Distribution. *International Journal of Astronomy and Astrophysics*, **13**, 154-165. https://doi.org/10.4236/ijaa.2023.133009

[39] Zaninetti, L. (2022) New Probability Distributions in Astrophysics: X. Truncation and Mass-Luminosity Relationship for the Frèchet Distribution. *International Journal of Astronomy and Astrophysics*, **12**, 347-362. https://doi.org/10.4236/ijaa.2022.124020

[40] Zaninetti, L. (2021) New Probability Distributions in Astrophysics: V. The Truncated Weibull Distribution. *International Journal of Astronomy and Astrophysics*, **11**, 133-149. https://doi.org/10.4236/ijaa.2021.111008

[41] Zaninetti, L. (2021) New Probability Distributions in Astrophysics: VI. The Truncated Sujatha Distribution. *International Journal of Astronomy and Astrophysics*, **11**, 517-529. https://doi.org/10.4236/ijaa.2021.114028

[42] Zaninetti, L. (2020) New Probability Distributions in Astrophysics: II. The Generalized and Double Truncated Lindley. *International Journal of Astronomy and Astrophysics*, **10**, 39-55. https://doi.org/10.4236/ijaa.2020.101004

[43] Zaninetti, L. (2013) A Right and Left Truncated Gamma Distribution with Application to the Stars. *Advanced Studies in Theoretical Physics*, **7**, 1139-1147. https://doi.org/10.12988/astp.2013.310125

[44] Olver, F.W.J., Lozier, D.W., Boisvert, R.F. and Clark, C.W. (2010) NIST Handbook of Mathematical Functions. Cambridge University Press.

Appendix A. Some Functions

The error function is defined by

$$\operatorname{erf}(x) = \frac{2}{\sqrt{\pi}} \int_0^x \mathrm{e}^{-t^2} \mathrm{d}t. \tag{A.1}$$

The complementary error function is

$$\operatorname{erfc}(x)x = \frac{2}{\sqrt{\pi}} \int_x^\infty \mathrm{e}^{-t^2} \mathrm{d}t = 1 - \operatorname{erf}(x), \tag{A.2}$$

see the handbook [44].